Research Journal of Engineering Sciences ISSN 2278 – 9472
Vol. **2(3),** 22-27, March **(2013)** *Res. J. Engineering Sci.*

The Stress Fields obtained from Strain Fields by Virtual Fields Method and Compared with Fem

Stamborská Michaela[1], Mares Vratislav[1] and Kvíčala Miroslav[2]
[1]Department of Material Engineering, Faculty of Metallurgy and Materials Engineering, VŠB-Technical University of Ostrava, 17. Listopadu, Ostrava – Poruba, CZECH REPUBLIC
[2]Department of Non-ferrous Metals, Refining and Recycling, Faculty of Metallurgy and Materials Engineering, VŠB-Technical University of Ostrava, 17. Listopadu, 70833 Ostrava, CZECH REPUBLIC

Available online at: www.isca.in
Received 20th February 2013, revised 5th March 2013, accepted 15th March 2013

Abstract

This paper presents comparison of the stress and strain fields gained by a digital image correlation (DIC) and FEM. This method was used to determine strain fields in narrow range of planar specimen. These strain fields were used for calculation of the stress fields by virtual fields method (VFM). The specimen was made from the hypoeutectoid ferrite-pearlite steel, which was used in production of train wheels. The analysis was carried out using two-dimensional DIC by which were obtained values of the strain fields. These values were measured on the surface of specimen in the elastic and plastic domain. Based on measured strain fields the stress fields were determined by Matlab software. Values obtained by this method were subsequently compared with those achieved by FEM.

Keywords: R7T steel, strain fields, stress fields, FEM, DIC, VFM.

Introduction

Many failures, which occurred in the past, were not caused by material behaviour, but due to the inappropriate design solutions i.e. bad technology, operating conditions, etc. It is generally known, that with the increasing material strength the weight of carrying elements can be significantly reduced. However, high strength does not guarantee the simultaneous increase of resistance to brittle fracture. The problem must be solved comprehensively and must respect the needs of classical mechanics, fracture mechanics, physical metallurgy, modern experimental and numerical methods. Knowledge of plastic material properties has a great significance, especially in the production of steel plates made by cold forming as well as in a prediction of elastic and plastic domains of carrying elements. It is beneficial to use DIC method during the loading of the specimen. This method allows to describe the strain fields over the entire surface and evaluate deformations in any point[1,2,3].

Hypoeutectoid steel R7T is used in the production of the railway wheels. The wheels are prone to contact fatigue. Fatigue crack propagates especially in ferrite across lamellar pearlite[4,5,6].

Research Methodology

The stress and strain analysis was realized on the planar specimen made from hypoeutectoid steel R7T. The steel characteristics are defined in the European Standard EN13262. Chemical composition of this steel was obtained by optical emission spectroscopy and is shown in Table-1

The steel was heat treated in the following way: austenitization at 850 °C/water cooling and tempering at 520°C. The mechanical properties were obtained from standard tensile tests of circular specimens, fracture toughness test and Vickers hardness test. Metallography was done by standard procedure (grinding - polishing and etching in a 3% Nital solution). Steel microstructure was studied by SEM. The experiment was realized on the planar specimen with geometry [mm], which is shown in the figure. 1.

Continuous movement of traverse was set during the tensile test on the machine Zwick/Roell 150. This movement of traverse was stopped in the predetermined displacement and the image was taken by camera Canon EOS 5D Mark II in the pause between displacements. The image data was further processed. Figure 2 shows diagram force – movement of traverse, this is a process of tensile test, where A and B are points, in which was the measurement realized.

Table-1
Chemical composition of R7T steel obtained by optical emission spectroscopy (wt. %).

C	Mn	Si	P	S	Cr	Ni	Mo	Cu	Ti	Al
0,385	0,824	0,496	0,007	0,003	0,24	0,074	0,010	0,01	0,001	0,022

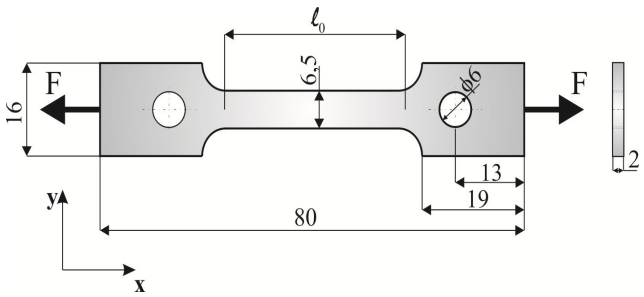

Figure-1
Geometry of the specimen [mm]

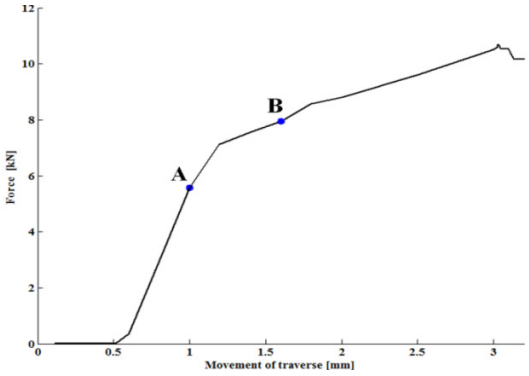

Figure-2
Diagram force – movement of traverse

The point A represents a point in the elastic domain, it is a state just below the yield stress and the point B is a point in the plastic domain when the yield stress is exceeded.

Due to the fact, that it was a plain analysis, measurement was realized with use of the only one sensing device, by which the displacement fields were obtained on the sample surface. The strain fields were calculated from displacement fields obtained by Vic 2D and compared with Abaqus, which is based on the FEM[7,8]. Stress fields were calculated in Matlab software after obtaining the parameters in an elastic and plastic domain. The results were compared with those obtained by Abaqus. Following setting was used for FEM simulations in Abaqus (quad-dominated element shape, standard element library, linear geometric order and approximate global size (0.5).

Results and Discussion

Microstructure and mechanical properties: Metallographic analysis showed that microstructure of R7T steel after tempering is made up of lamellar pearlite with the ferritic networking (figure. 3)

Selected microstructural characteristics, such as grain size and interlamellar distance, and mechanical properties were determined using tensile test, fracture toughness test and Vickers hardness test (table. 2).

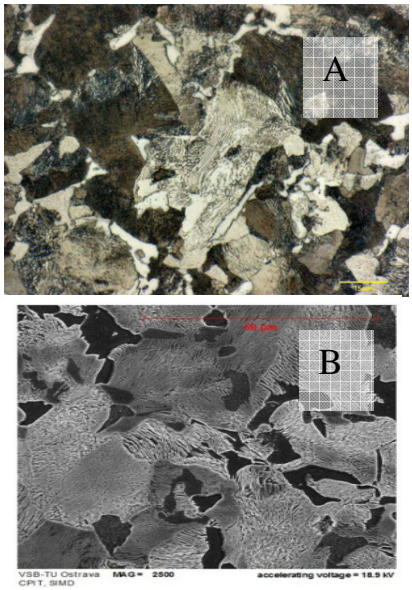

Figure-3
R7T steel microstructure–A, lamellar pearlite – B

Table-2
Selected microstructural and mechanical properties of R7T steel.

Grain size - EN ISO 643 [G]	10
Interlamellar distance [μm]	0.53
$R_{p0.2}$ [MPa]	515
R_m [MPa]	837
A_{10} [%]	14,1
Hardness [HV_{10}]	228
Fracture toughness K_{IC} [MPa* $m^{1/2}$]	87.96

Abaqus simulations: The results of the stress and strain fields obtained by Abaqus simulation are expressed as the strain fields ε_x, ε_y and γ_{xy} for specimen in the elastic domain (point A), see figure-4.

Elastic range **Plastic range**

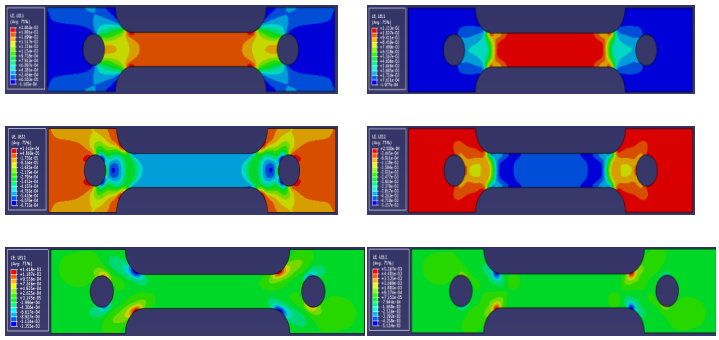

Figure-4
The strain fields ε_x, ε_y and γ_{xy} in elastic and plastic range obtained by FEM

The same calculations were performed for the stress fields σ_x, σ_y and τ_{xy} in the plastic domain (point B), see figure. 5.

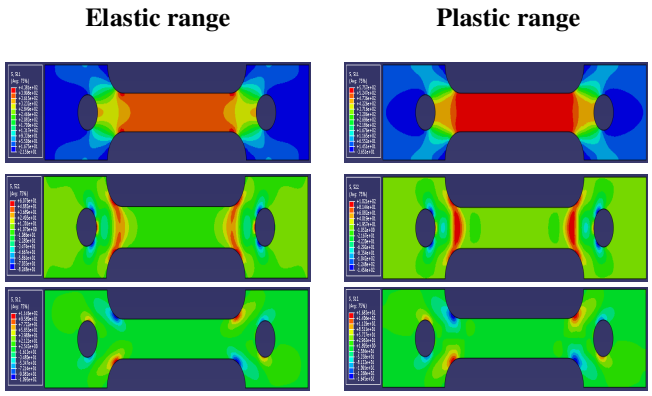

Figure-5
The stress fields σ_x, σ_y and τ_{xy} in elastic and plastic range obtained by FEM

Vic 2D simulations: The object deformations are observed by camera vertically aimed at a surface in a case of plain DIC analysis. Figure 6 shows the schematic illustration of a typical experimental setup using an optical imaging device for the 2D DIC method[9,10].

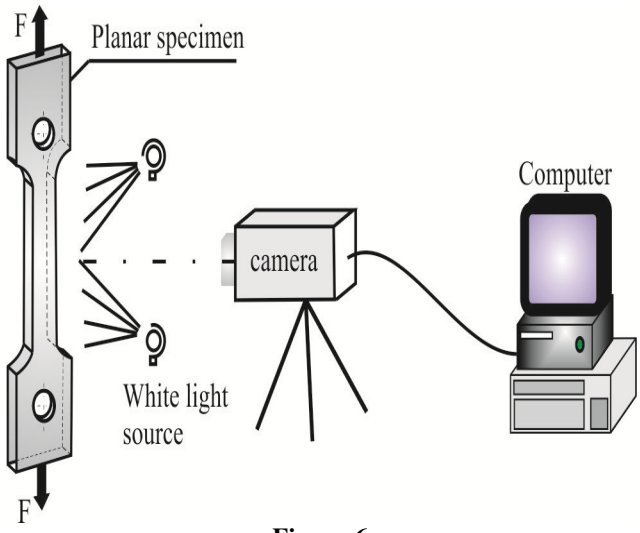

Figure-6
Principe of 2D digital image correlation

The software Vic 2D was used to evaluate the measurement results. The correlation algorithm was running with a use of correlation window composed of 27 pixels and with a 5 pixel step between two measurement points. The incremental correlation option was used, i.e. each image is correlated with the previous one, and the measured incremental displacement is added to the one measured in the previous step. The strain fields ε_x, ε_y and γ_{xy} in an elastic range obtained by Vic 2D for point A, are shown in the figure-7

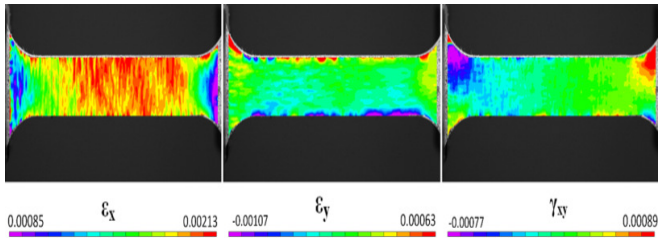

Figure-7
The strain fields ε_x, ε_y and γ_{xy} in elastic range obtained by Vic 2D

The yield stress of the material is not exceeded at the position of a point A. On the contrary, the strain fields ε_x, ε_y and γ_{xy} exceeded yield stress in plastic range at the position of a point B, see figure. 8.

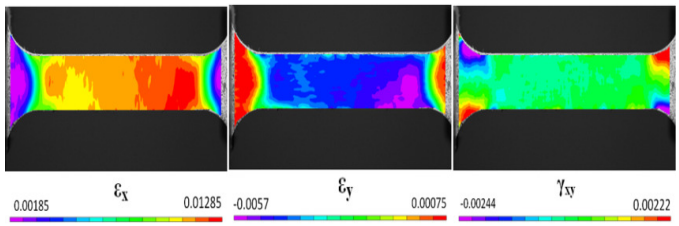

Figure-8
The strain fields ε_x, ε_y and γ_{xy} in plastic range obtained by Vic 2D

The values of strain fields obtained by Vic 2D correspond to results calculated by Abaqus.

The virtual fields method: The strain fields ε_x, ε_y and γ_{xy} were calculated from the displacements u_x and u_y by Camfit. In the elasto-plastic region, the Camfit uses only one constant virtual strain field, as defined previously it depends on the test configuration. It can also be seen as the difference between averages, normal or shear force, measured and recalculated from the strains and the constitutive parameters[11,12,13]. The program first identifies the isotropic elastic constants, as it can be seen in figure. 10 a). This enables to define an elastic range for the test, due to the plot which reports external and internal virtual work. If linearity is correct, then the elastic range was defined properly. Otherwise, it should be changed to achieve to acceptable linearity.

The second stage concerns the plastic parameters and four isotropic hardening models, such as a simple Prandtl-Reuss model. In this case the power law model was chosen and the results are shown in figure. 10b)[14,15,16].

Stress field identification from strain field using the VFM: The generalized Hooke's law was used to calculate stress fields in the elastic range. The plastic parameters obtained by Camfit were used for calculation of the stress fields

$$\sigma_{H(k)} = K.(\varepsilon_0 + \varepsilon_{eq_{pl}(k)})^n \quad (1)$$

where $\sigma_{H(k)}$ is the equivalent stress, $k-$ is the step of measurement, $\varepsilon_{eq_{pl}(k)}$ - is the equivalent of accumulated plastic strain, K, ε_0, n - are the parameters obtained by Camfit.

The equivalent of accumulated plastic strain was calculated according to equation. 2

$$\varepsilon_{eq_{pl(k)}} = \sqrt{\frac{2}{3}\left(2\varepsilon_{x(k)}^2 + 2\varepsilon_{y(k)}^2 + 2\varepsilon_{x(k)}\varepsilon_{y(k)} + \frac{\gamma_{xy(k)}^2}{2}\right)}, \quad (2)$$

where $\varepsilon_{x(k)}, \varepsilon_{y(k)}, \gamma_{xy(k)}$ are the values of strain fields obtained by measurement of displacement fields on the specimen´s surface for k- steps with use of DIC. The stress fields σ_x, σ_y and τ_{xy} in the elastic range obtained by Matlab (point A) are shown in the figure. 11.

Analogically, the stress fields σ_x, σ_y and τ_{xy} in the plastic range (point B) are demonstrated in the figure. 12.

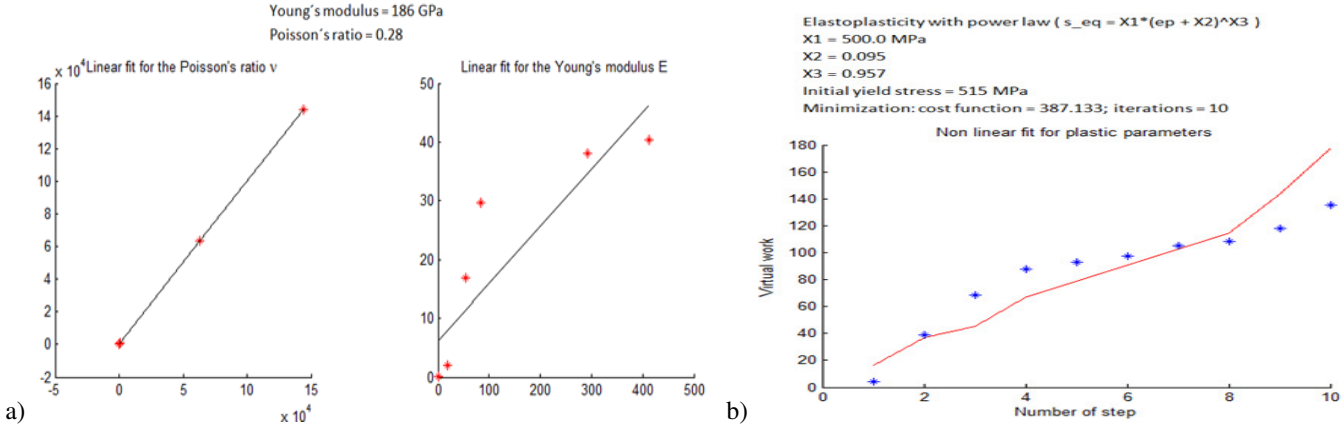

Figure-10
Parameters obtained in a) elastic range, b) plastic range by Camfit

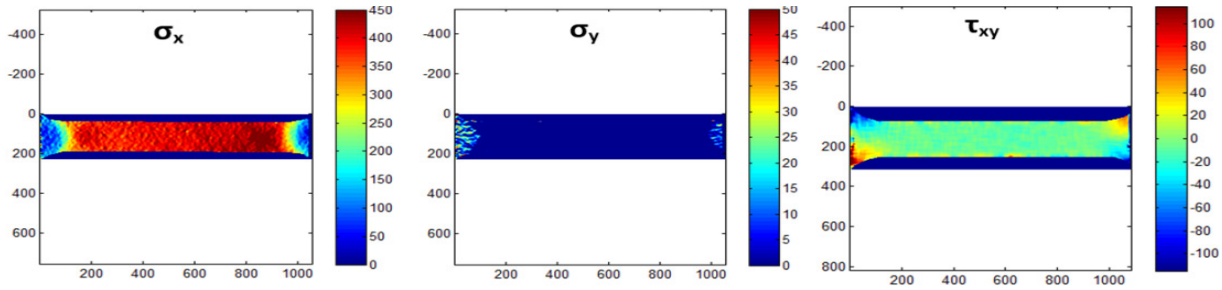

Figure-11
The stress fields σ_x, σ_y a τ_{xy} [MPa] in elastic range obtained by Matlab

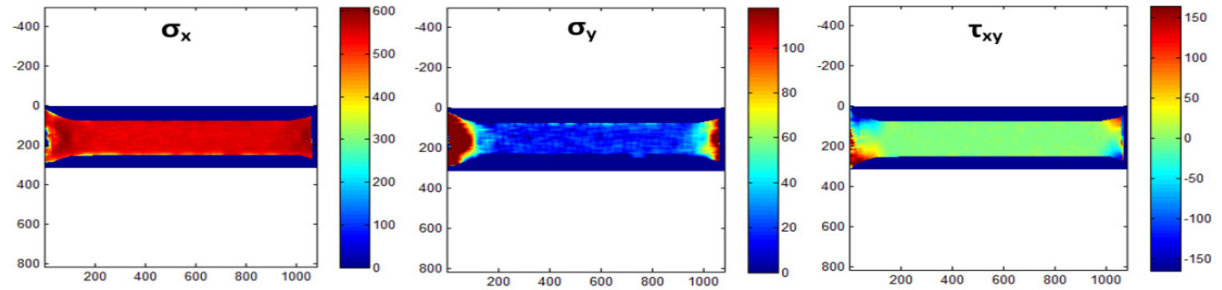

Figure-12
The stress fields σ_x, σ_y a τ_{xy} [MPa] in plastic range obtained by Matlab

The values of strain fields obtained by Matlab correspond to results calculated by Abaqus.

Methods comparison: It can be noticed, that there are no significant differences between the strain fields results obtained by DIC and FEM in the elastic range. The values gained by FEM are $\varepsilon_x = 1{,}881.10^{-3}$, $\varepsilon_y = -5.420x10^{-4}$, $\gamma_{xy} \approx 0$ and the values by DIC are $\varepsilon_x = 1.89x10^{-3}$, $\varepsilon_y = (-3.26 \div -5.3875)x10^{-4}$, $\gamma_{xy} \approx 0$.

The results of stress fields obtained by FEM in the elastic range were $\sigma_x \approx 400$ MPa, $\sigma_y \approx 0$ MPa, $\tau_{xy} \approx 0$. The generalized Hooke's law was used to calculate stress fields by Matlab in the elastic range and the results of stress fields were $\sigma_x \approx 420$ MPa, $\sigma_y \approx 0$ MPa, $\tau_{xy} \approx 0$. It can be noticed, that the values σ_y obtained by MATLAB equal zero in the central part of the specimen and therefore this part disappeared in the picture.

From the comparison, it can be seen, that there are only marginal differences in the strain fields results determined by FEM - $\varepsilon_x = 1.133x10^{-2}$, $\varepsilon_y = -4.258x10^{-3}$, $\gamma_{xy} \approx 0$ and the values by DIC $\varepsilon_x = 1.1475x10^{-2}$, $\varepsilon_y = -4.49063x10^{-3}$, $\gamma_{xy} \approx (-4.0 \div 4.0)x10^{-4}$. The only one significant difference was observed in case of the γ_{xy}. The results of stress fields obtained by FEM in the plastic range were $\sigma_x = 575.7$ MPa, $\sigma_y = 19.57$ MPa, $\tau_{xy} \approx 0$. The hardening law was used to calculate stress fields by Matlab in the plastic range and the results of stress fields were $\sigma_x \approx 580$ MPa, $\sigma_y \approx 20$ MPa, $\tau_{xy} \approx 0$.

Conclusion

The experiment was realized on the planar specimen with coordinate system chosen so that the load was oriented in the direction of the sample's x-axis. Due to the fact, that it was a plain analysis, measurement was realized using the only one sensing device, by which the displacement fields were obtained on the sample surface.

Co mparing these methods (FEM – DIC - VFM), it can be said, that the good agreement has been achieved. The problem might be caused by the color application to the edge of the specimen. In this case, DIC software Vic 2D does not calculate strain fields properly, and those are considered to be a marginal effect.

It is possible to use two dimensional measurement to solve the planar tasks with a sufficient accuracy. It is appropriate to note, that when the measurement is realized with just one camera, this camera must be precisely orientated in perpendicular direction to the surface of the sample

Acknowledgements

This article has been elaborated in the framework of the project Opportunity for young researchers, reg. no. CZ.1.07/2.3.00/30.0016, supported by Operational Programme Education for Competitiveness and co-financed by the European Social Fund and the state budget of the Czech Republic and in the framework of the project Regional Materials Technology Research Centre (RMTVC) reg. no.: CZ.1.05/2.1.00/01.0040.

References

1. Purkar T.S. and Pathak S., Analysis of Crack Initiation in Fretting Fatigue Specimen, *ISCA J. Engineering Sci.*, **1(1),** 26-34 **(2012)**

2. Lakshmanan N., Ramachandran G.M. and Saravanan K., Dynamic Stress Analysis of a Multi cylinder Two-stage Compressor Crankshaft, *Research J. Engineering Sci*., **1(4)**, 34-40 **(2012)**

3. Lakshmanan N. and Saravanan K., Cause and Effect Assessment after a Complex Failure of a Trunk Piston in Oil Free Compressor, *Research J. Engineering Sci.*, **1(6)**, 56-60 **(2012)**

4. Nikhil D. and Vivek S., Graph Theoretic approach (GTA) A Multi-Attribute Decision Making (MADM) Technique Attri Rajesh, *Res. J. Engineering Sci.*, **2(1)**, 50-53 **(2013)**

5. Sreenivasulu R. and Rao Ch. S., Design of Experiments based Grey Relational Analysis in Various Machining Processes - A Review, *Res. J. Engineering Sci*., **2(1)**, 21-26 **(2013)**

6. Gmiterko A.K. and Virgala M.I., The snake rectilinear motion modeling on the flat in clined surface, *International Journal of Mechanics and Applications*., **2(4)**, 39-42, **(2012)**

7. Holzmann M., Jurášek L. and Dlouhý I., Fracture behaviour and cleavage initiation in hypoeutectoid pearlitic steel, *International Journal of Fracture*, **148**, 13-28 **(2007)**

8. Zaretsky E.V., Rolling bearing steels a technical and historical perspective, *Materials Science and Technology*, **28**, 58-69, **(2012)**

9. Abouridouane M., Klocke F., Lung D. and Adams O., A new 3D multiphase FE model for micro cutting ferritic–pearlitic carbon steels, *CIRP Annals - Manufacturing Technology*, **61,** 71–74 **(2012)**

10. Ghadbeigi H., Pinna C. and Celotto S., Quantitative Strain Analysis of the Large Deformation at the Scale of Microstructure: Comparison between Digital Image Correlation and Microgrid Techniques *Experimental Mechanics,* **52**, 1483-1492 **(2012)**

11. Rossi M. and Pierron F., Identification of plastic constitutive parameters at large deformations from three dimensional displacement fields, *Comput Mech,* **49,** 53-71 **(2012)**

12. Sozen S. and Guler M., Determination of displacement distributions in bolted steel tension elements using digital

image techniques, Optics and Lasers in Engineering, **49**, 1428–1435 **(2011)**

13. Sutton M.A., Orteu J.J. and Schreier H.W., Image correlation for shape, motion and deformation measurements, *Springer* **(2009)**

14. Štamborská M., Šimčák F., Kalina M. and Schrötter M., Identification of the Stress Fields from the Strain Fields in the Isotropic Materials, *Procedia Engineering*, **48**, 665-672 **(2012)**

15. Tarantino M.G., Beretta S., Foletti S. and Papadopoulos I., Experiments under pure shear and rolling contact fatigue conditions: Competition between tensile and shear mode crack growth, *International Journal of Fatigue,* **46**, 67-80 **(2013)**

16. Wang J., Levkovitch V., Reusch F., Svendsen B., Huétink J. and Van Riel M., On the modeling of hardening in metals during non-proportional loading, *International Journal of Plasticity*, **24(6),** 1039-1070 **(2008)**